High-pressure phase transformation of the silicon clathrate Si_{136}

High-pressure phase transformation of the silicon clathrate Si$_{136}$

Ganesh K Ramachandran†‡, Paul F McMillan†‡, Sudip K Deb‡¶,
Maddury Somayazulu‡$^+$, Jan Gryko§, Jianjun Dong‖ and Otto F Sankey‖

† Department of Chemistry and Biochemistry, Arizona State University, Tempe, AZ 85287, USA
‡ Center for Solid State Science, Arizona State University, Tempe, AZ 85287, USA
§ Department of Earth and Physical Sciences, Jacksonville State University, AL 36235, USA
‖ Department of Physics and Astronomy, Arizona State University, Tempe, AZ 85287, USA

E-mail: `krg@asu.edu` (G K Ramachandran)

Abstract. The compressional behaviour of a new *expanded* form of silicon, the cubic Si$_{136}$ clathrate, is studied by energy dispersive x-ray diffraction in a diamond anvil cell experiment. The ambient temperature bulk modulus and its pressure derivative are determined to be $K_0 = 90(3)$ GPa and $K'_0 = 5.2(8)$, in agreement with LDA theoretical calculations. At pressures between 8 and 10 GPa, the structure transforms into the thermodynamically stable β-Sn phase. This behaviour is analogous to that of diamond-structured silicon. However, the metastable transition from Si$_{136}$ to the β-Sn structure should occur at a much lower pressure (3–4 GPa), from consideration of free energy–pressure relations. The observation can be related to the absence of a convenient low-energy pathway for the IV- to VI-fold coordination change involved in the transition from Si$_{136}$ to β-Sn.

Open framework structures of the group IV elements silicon, germanium and tin have been known for the last three decades [1–3]. It was recognized during the early works that these materials are analogous to the clathrate hydrates [4], which form when water molecules arrange in cagelike structures around gas or solvent molecules. The group IV elements form the basis for condensed *fullerane*-like polyhedral units consisting of five- and six-membered rings. Fusing polyhedra of different sizes through the five- and six-membered rings results in extended Si, Ge or Sn based clathrate structures. Alkali or alkali-earth atoms which are invariably used in the synthesis of these clathrates [1–3], reside endohedrally inside the polyhedra formed by the group IV atom, and are believed to have the role of stabilizing the overall structure. For silicon, two clathrate structures have been experimentally identified [1–3] to date: M$_x$Si$_{136}$ ($0 < x < 24$) and M$_x$Si$_{46}$ ($0 < x < 8$). A variety of guest atoms (M) ranging from sodium to barium [5] have been used to successfully synthesize these materials. The discovery of superconductivity in the Na$_x$Ba$_y$Si$_{46}$ based clathrates [6] and the important theoretical prediction that Si$_{136}$ could be an useful optical material [7], as well as their potential as thermoelectric materials [8], has created much interest in these unique phases. The material studied here is new in that we have recently achieved [9] complete removal of the encapsulated Na atoms from Na$_x$Si$_{136}$ to yield an *expanded semiconductor* Si$_{136}$, with a wide bandgap of ~2 eV. There have been extensive studies of the behaviour of diamond structured silicon (d-Si) at high pressure, with a range of stable and metastable transitions to octahedral and tetrahedral

¶ On leave from Solid State Physics Division, Bhabha Atomic Research Center, Bombay 400085, India.
$^+$ Also at the Geophysical Laboratory, Carnegie Institute of Washington, DC, USA.
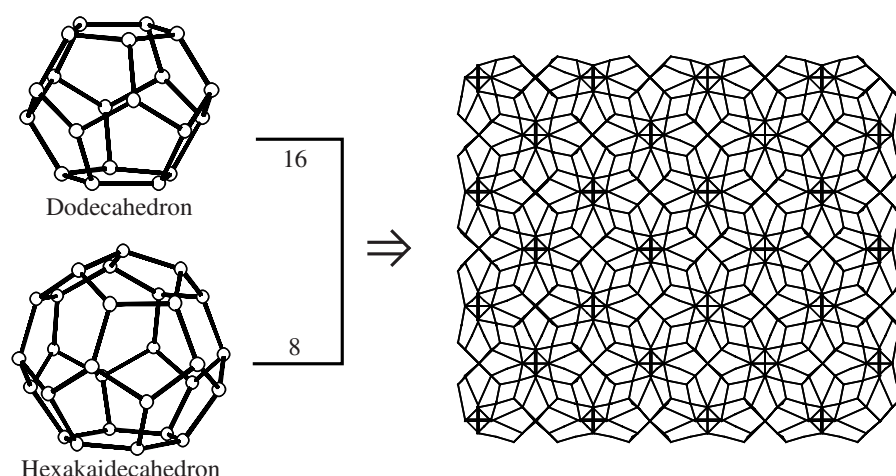
Figure 1. Skeletal models for the building blocks of the silicon clathrate Si_{136}. A *dodecahedron* is a 20-atom polyhedron (Si_{20}) and has 12 faces while the *hexakaidecahedron* is a 28-atom polyhedron (Si_{28}) with 16 faces. Fusing Si_{20} with Si_{28} in the ratio 16:8 through five- and six-membered rings results in the expanded volume phase, Si_{136}, which crystallizes in the cubic $Fd\bar{3}m$ space group. Note the large number of five-membered rings and also the presence of planar six-membered rings in the motifs. Shown on the right is a projection of the structure along the (001) direction. For additional stereographs of the structure see [20].

structures upon compression and decompression [10–15]. Work on silicon nanoparticles [16] and on porous silicon [17–19] has shown that the surface free energy plays a critical role in determining the onset pressure and observed sequence of transitions. It is of interest then, to examine the structural behaviour of Si_{136}, to observe the phase transition behaviour of this tetrahedral framework structure with internal 'pores' and a bonding topology distinctly different from that of diamond (see figure 1 for building blocks and a perspective of the Si_{136} structure).

Normal d-Si undergoes a well characterized sequence of transformations upon pressurization at ambient temperature. Beginning at about 8 GPa it transforms into the body centred tetragonal structure of β-Sn [11–14]. This phase contains Si atoms in an octahedral coordination, and is metallic. The transition is first order, and the stable reaction boundary occurs at approximately 7–8 GPa at ambient temperature [11–14]. Most studies find the completion of transition by 10–12 GPa. At ~15 GPa, the β-Sn structure undergoes a displacive transition to a metallic simple hexagonal (sh) structure. There is also evidence for a further phase between and β-Sn and the sh phase [13]. Further application of pressure on silicon realizes a sequence of orthorhombic [15] and hexagonally close packed (hcp) structures before a final transformation into a dense cubic close packed (ccp) structure at 78 GPa [12]. Upon decompression, the β-Sn phase is retained to approximately 1 GPa, upon which it transforms to a metastable body centred cubic (BC8) form of silicon [10]. Heating this decompressed material causes a metastable transition to the hexagonal diamond (lonsdaleite) form [10]. Other metastable tetrahedral forms have also been reported at ambient pressure, depending upon the recovery conditions from high pressure. The behaviour of nanocrystalline and porous silicon (p-Si) is different. Depending upon the nanocrystallite size, the transition to the β-Sn structure is suppressed, and a transition to the sh phase occurs directly at ~14 GPa [16]. Raman spectroscopic studies of p-Si show that the signal of the tetrahedral semiconducting material is lost at 14–18 GPa [17–19]. It has been suggested that some parts of the sample transform to β-Sn, but this is not borne out by recent diffraction measurements [28].

The alkali-free silicon clathrate Si$_{136}$ was prepared by thermal decomposition of the Zintl phase NaSi, followed by progressive vacuum heating and density separation, as described elsewhere [20]. The sample was loaded into a Mao–Bell type diamond cell, with anvils having 350 μm culets. The sample chamber was formed by drilling a 120 μm hole in a T301 steel gasket. A 4:1 methanol–ethanol mixture was used as the pressure transmitting fluid. The pressure was measured using the ruby fluorescence scale [21] ($d\lambda/dP = 0.365$ nm GPa^{-1}). Energy dispersive x-ray diffraction patterns were collected at the superconducting wiggler beam line station X17-C of the National Synchrotron Light Source (NSLS). Data were collected at the diffracting angle of $2\theta = 15.00(5)°$.

In figure 2, we plot selected energy dispersive x-ray diffraction patterns for Si$_{136}$ as a function of pressure. Up to ~8 GPa, all peaks can be indexed to the reflections from the face-centred $Fd\bar{3}m$ cell of Si$_{136}$, well known from ambient pressure studies [20, 22]. The lattice parameter was obtained from the data as a function of pressure using the Lebail extraction technique available in the GSAS [23] program. The variation of cell volume with pressure is shown in figure 3, along with a Birch–Murnaghan fit to the data assuming $K_0' = 4.00$. This yields an estimated bulk modulus $K_0 = 87(3)$ GPa. Also shown are results of an LDA calculation [24] for the Si$_{136}$ phase, which yield $K_0 = 81.2$ GPa for $K_0' = 4.45$. The systematic 1.6% difference in volume between theory and experiment can be partly ascribed to thermal expansion, since the calculations were performed at 0 K. In order to obtain a better estimate for the bulk modulus and its pressure derivative, we used an Eulerian finite-strain method to fit a Birch–Murnaghan equation of state [25, 26]. For this analysis, a measure of the negative Eulerian strain, f_v,

$$f_v = \tfrac{1}{2}[(V/V_0)^{-2/3} - 1]$$

and a normalized pressure, F,

$$F = P[3f_v(1 + 2f_v)^{2.5}]^{-1}$$

are defined. Then the Birch–Murnaghan EoS is written as

$$F = K_0[1 - \tfrac{3}{2}(4 - K_0')f_v]$$

and the parameters K_0 and K_0' are readily extracted from a plot of F against f_v (figure 4). A least squares best fit to our data yields $K_0 = 90(3)$ GPa and $K_0' = 5.2(8)$, table 1. In table 2 are listed the observed and calculated reflections for the phase at a pressure of 2 GPa.

On pressurization above 8 GPa, the diffraction pattern is dominated by lines from the β-Sn phase (figure 2). The transition is essentially complete by 10.3 GPa, and the sample has fully transformed at 12 GPa. The strongest lines in the diffraction pattern at 10.3 GPa are indexed to the (200), (101), (220) and (121) peaks of the high pressure tetragonal β-tin structure of silicon with $a = 4.6813(1)$ Å and $c = 2.5884(1)$ Å, which lie within the range reported for lattice parameters of this material in the transition range [11–14]. There is then a very large (~33%) volume change at the transition from the Si$_{136}$ phase, compared with that from d-Si (~22%) into the same phase [11–14].

It is interesting that the metastable transition to the β-Sn phase should occur in the same pressure range as for diamond structured silicon. In figure 5, we plot a theoretical free

Table 1. Summary of high pressure parameters from a Birch–Murnaghan equation of state analysis.

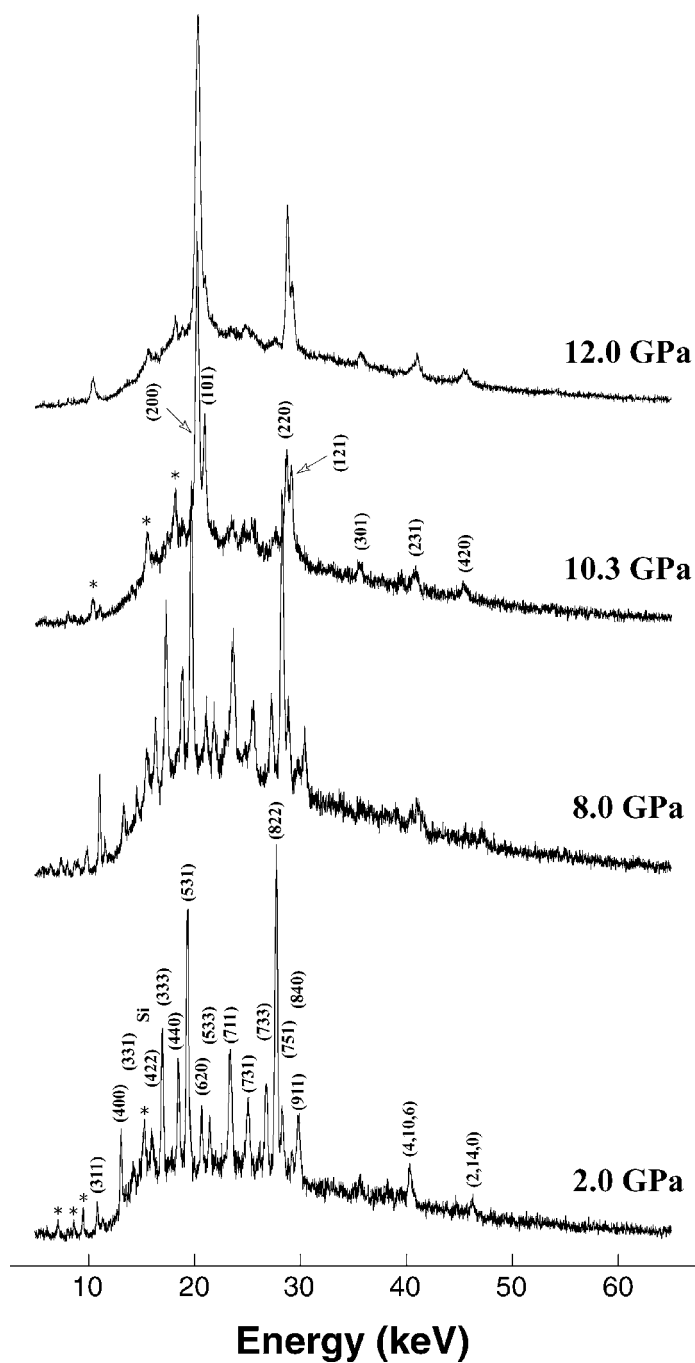|	V_0 (Å^3/atom)	K_0 (GPa)	K_0'
Experiment	23.01	90(3)	5.2(8)
Theory	22.65	81.15	4.45

Figure 2. Evolution of the x-ray diffraction pattern of Si_{136} as a function of pressure. The phase transformation to the dense β-tin structure occurs between 8.0 and 10.3 GPa. The strongest lines at 10.3 GPa could be attributed to the (200), (101), (220) and (121) reflections from the high pressure tetragonal β-tin structure of silicon with $a = 4.6813(1)$ Å and $c = 2.5884(1)$ Å. Similar data collected at 12.0 GPa (topmost curve) could also be indexed to the β-tin structure. The peak identified by a star at 2 GPa corresponds to the (111) reflection from some residual d-Si. All peaks identified below 10 keV correspond to fluorescence lines. 'Escape' peaks are also identified in the pattern at the pressure of 10.3 GPa.
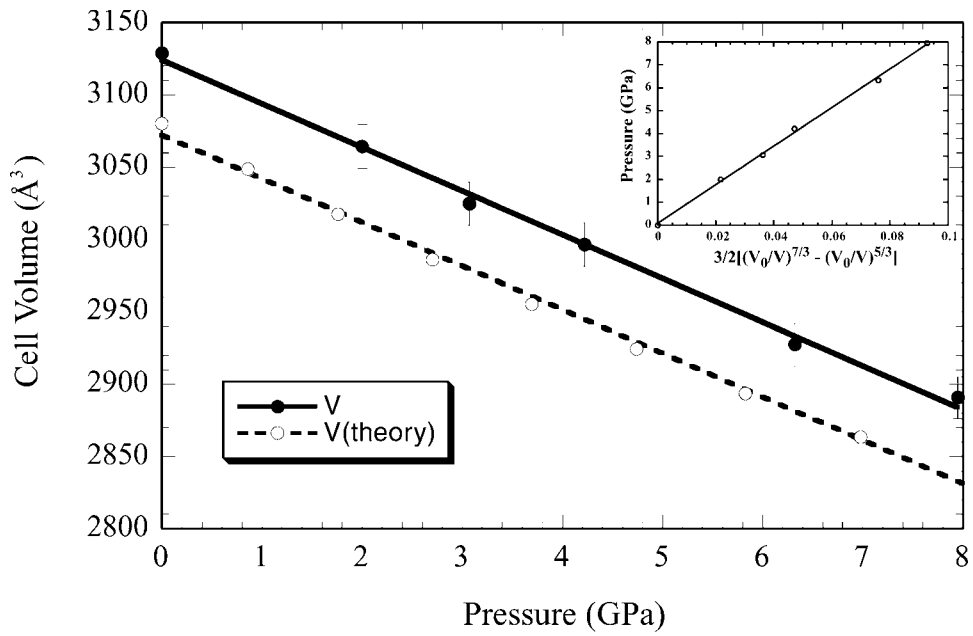
Figure 3. Pressure dependence of the unit cell volume in Si$_{136}$. Both experimental data and theoretical data (from LDA calculations) are shown. Over the pressure range shown, Si$_{136}$ undergoes a $\sim$7.5% volume change. In the inset, pressure is plotted against reduced volume (Birch–Murnaghan assuming $K_0' = 4.0$). This resulted in a value $K_0 = 87(3)$ GPa.
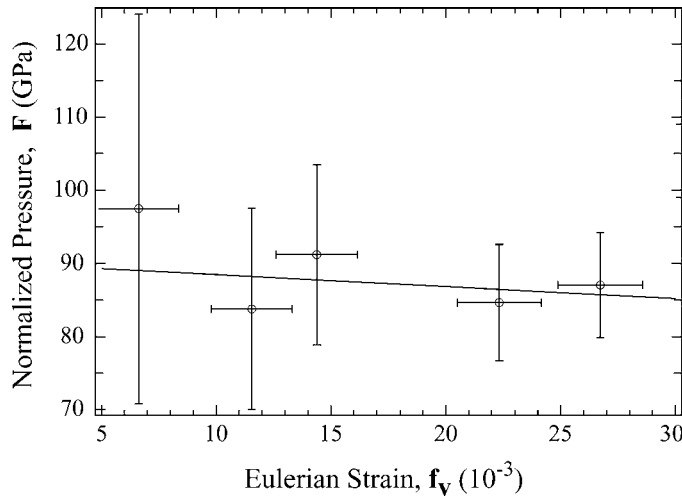

Figure 4. An F–f_v plot for data from figure 3, fitted to a third-order Birch–Murnaghan equation of state using the Eulerian-strain method (see text for explanation) gave a bulk modulus $K_0 = 90(3)$ GPa and its pressure derivative $K_0' = 5.2(8)$.

energy–pressure diagram for the three phases. The slope of the plot at any pressure for a given phase is its atomic volume (per Si atom), and the curvature is proportional to its compressibility. At ambient pressure and temperature d-Si is the most stable form, and its free energy curve crosses that of the β-Sn form at $\sim$8 GPa. The transition is first order, however, and ambient-

Table 2. Observed and calculated reflections for Si_{136} at 2.00 GPa.

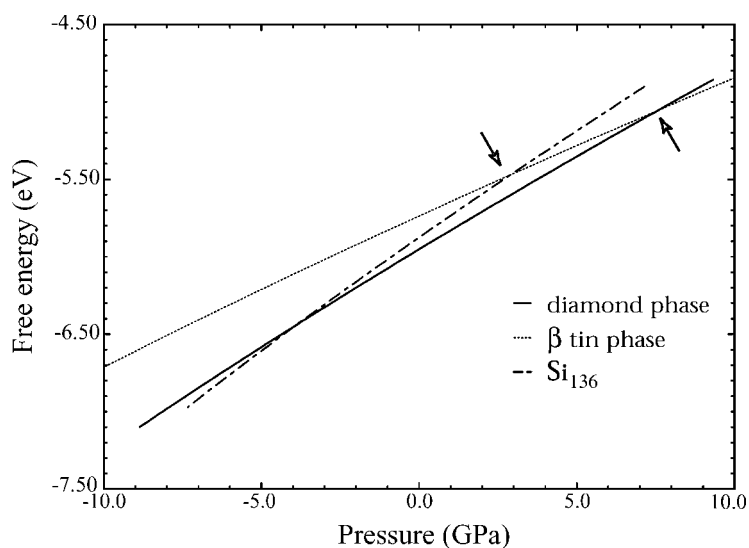| E (keV)	d_{obs} (Å)	d_{cal} (Å)	(hkl)
10.8	4.3976	4.38	(311)
13.1	3.6255	3.63	(400)
14.2	3.3447	3.33	(331)
15.9	2.9871	2.97	(422)
17.0	2.7938	2.80	(333)
18.4	2.5812	2.57	(440)
19.4	2.4482	2.46	(531)
20.7	2.2944	2.30	(620)
21.4	2.2194	2.22	(533)
23.4	2.0297	2.04	(711)
25.1	1.8922	1.89	(731)
26.7	1.7788	1.78	(733)
27.8	1.7084	1.71	(822)
28.3	1.6782	1.68	(751)
29.2	1.6265	1.63	(840)
29.9	1.5894	1.60	(911)
40.3	1.1785	1.18	(4, 10, 6)
46.3	1.0331	1.03	(2, 14, 0)

Figure 5. Theoretical (LDA) free energy–pressure plot for the three phases d-Si, Si_{136} and β-tin. The slope of the plot at any pressure for a given phase is its atomic volume (per atom), and the curvature is proportional to its compressibility. Theory predicts a transition pressure of 8 GPa for the d-Si to β-tin transition (arrow pointing up) which is in excellent agreement with experiments [11–14]. However, theory predicts a much lower (3–4 GPa, arrow pointing down) pressure for the Si_{136} to β-tin transition which is experimentally observed between 8.0 and 10.3 GPa. We argue in the text that the absence of a convenient low-energy pathway for the Si_{136} to β-tin transition is the reason for this discrepancy.

temperature compression at normal laboratory timescales results in the first observation of the onset of the transition at $\sim$8 GPa. Continued compression at the same rate results in the completion of the phase change by $\sim$12 GPa. In the case of the expanded Si_{136} phase, the

ambient volume is much larger than that for d-Si, so that the slope of the free energy–pressure plot is larger. In addition, it is estimated from LDA calculations [24, 27] that the clathrate phase lies ∼75 meV (3 kT, or ∼7.50 kJ mol^{-1}) above d-Si at ambient pressure. The result is that the LDA determined free energy–pressure curve for Si$_{136}$ will cross that of the stable diamond phase at 'negative' pressure (-3 to -4 GPa) in a tensile regime, and will metastably encounter that of β-Sn at 3.5 GPa; i.e. at a much lower pressure than does the diamond phase. We thus expect the metastable Si$_{136}$ $\leftrightarrow$ β-Sn transformation to occur at significantly lower pressure, from free energy considerations. In our study, however, we observe the onset of this transition between 8 and 10 GPa, with completion at ∼12 GPa.

This observation strongly suggests that the Si$_{136}$ $\leftrightarrow$ β-Sn transition is kinetically impeded compared with that between d-Si and the β-Sn structure. The phase transformation from diamond to the high-pressure β-Sn structure can be easily visualized in terms of a tetragonal (along the c-axis) distortion of the unit cell accompanied by flattening of the fused cyclo-hexane rings. Although the transition is first order, there is an 'easy' transition pathway that involves co-operative bond formation and lengthening, with no covalent bond breaking or large atomic rearrangements necessary. The resulting activation energy is low, and at ambient temperature the transition is readily completed within a laboratory time scale (minutes to hours), over a moderate pressure range (8–12 GPa) only slightly above the thermodynamic transition pressure. In contrast to this situation, the Si$_{136}$ phase contains slightly distorted tetrahedral Si atoms arranged into planar five- and six-membered rings (see figure 1), and no part of the structure resembles the topology of diamond. There is thus no analogous 'easy' pathway into the β-Sn structure, and indeed substantial Si–Si bond breaking coupled with large displacements of the Si atoms must occur for the dense octahedral β-Sn structure to be obtained. We believe that these considerations account for a greatly increased activation energy for the Si$_{136}$ $\leftrightarrow$ β-Sn transition compared with that from the diamond structured phase, and hence the observation that the onset of the transformation is observed at much higher pressures than expected. Once initiated, however, the larger $-P\Delta V$ term associated with the transition from the clathrate phase provides an additional energetic driving force, that must aid in promoting completion of the metastable phase transition. Further theoretical work is under way to explore the energetics of the transformation pathway.

Note added in proof. In the meanwhile we have become aware of a similar high pressure study of a sodium bearing clathrate, Na$_{0.6}$Si$_{136}$, by San-Miguel *et al* (1999 *Phys. Rev. Lett.* **83** 5290). They report a transformation into the β-tin structure as well, but at a slightly higher transition pressure (11 GPa). At least for low sodium contents, this perhaps suggests an influence of the Na content on the phase transition pressure—the larger the sodium content the larger the transition pressure.

References

[1] Kasper J S, Hagenmuller P, Pouchard M and Cros C 1965 *Science* **150** 1713
[2] Cros C, Pouchard M and Hagenmuller P 1970 *J. Solid State Chem.* **2** 570
[3] Cros C, Pouchard M, Hagenmuller P and Kasper J S 1968 *Bull. Soc. Chim. Fr.* **7** 2737
[4] Pauling L and Marsh R E 1952 *Proc. Natl Acad. Sci. USA* **38** 112
[5] Yamanaka S, Horie H-O, Kawaji H and Ishikawa M 1995 *Eur. J. Solid State Inorg. Chem.* **32** 799
[6] Kawaji H, Horie H-O, Yamanaka S and Ishikawa M 1995 *Phys. Rev. Lett.* **74** 1427

[7] Adams G B, O'Keeffe M, Demkov A A, Sankey O F and Huang Y-M 1994 *Phys. Rev.* B **49** 8048

[8] Cohn J L, Nolas G S, Fessatidis V, Metcalf T H and Slack G A 1999 *Phys. Rev. Lett.* **82** 779

[9] Gryko J, McMillan P F, Marzke R F, Ramachandran G K, Patton D, Deb S K and Sankey O F 1999 *Science* submitted

[10] Wentorf R M and Kasper J S 1963 *Science* **139** 338

[11] Hu J Z, Merkle L D, Menoni C S and Spain I L 1986 *Phys. Rev.* B **34** 4679

[12] Duclos S J, Vohra Y K and Ruoff A L 1990 *Phys. Rev.* B **41** 12 021

[13] McMahon M I and Nelmes R J 1993 *Phys. Rev.* B **47** 8337

[14] Imai M, Mitamura M, Yaoita K and Tsuji K 1996 *High Pres. Res.* **15** 167

[15] Hanfland M, Schwarz U, Syassen U and Takemura K 1999 *Phys. Rev. Lett.* **82** 1197

[16] Tolbert S H, Herhold A B, Brus L E and Alivisatos A P 1996 *Phys. Rev. Lett.* **76** 4384

[17] Zeman J, Zigone M, Rikken G L G A and Martinez G 1995 *J. Phys. Chem. Solids* **56** 655

[18] Papadimitriou D, Raptis Y S and Nassiopoulou A G 1998 *Phys. Rev.* B **58** 14 089

[19] Papadimitriou D, Raptis Y S, Nassiopoulou A G and Kaltsas G 1998 *Phys. Status Solidi* a **165** 43

[20] Ramachandran G K, Dong J, Diefenbacher J, Gryko J, Marzke R F, Sankey O F and McMillan P F 1999 *J. Solid State Chem.* **145** 716

[21] Mao H-K, Xu J and Bell P M 1986 *J. Geophys. Res.–Sol. Earth Plan.* **91** 4673

[22] Reny E, Gravereau P, Cros C and Pouchard C 1998 *J. Mater. Chem.* **8** 2839

[23] Larson A C and von Dreele R B 1989 *GSAS: Generalized Structure Analysis System* LANSCE, MS-H805, Manual Lujan Neutron Scattering Center, Los Alamos, NM

[24] Dong J, Sankey O F and Kern G 1999 *Phys. Rev.* B **60** 950

[25] Birch F J 1978 *J. Geophys. Res.* **83** 1257

[26] Murnaghan F D 1944 *Proc. Natl Acad. Sci. USA* **30** 244

[27] O'Keeffe M, Adams G B and Sankey O F 1998 *Phil. Mag. Lett.* **78** 21

[28] Deb *et al* in preparation